

Robust energy management of a microgrid with photovoltaic inverters in VAR compensation mode

Iman Goroohi Sardou^{a,*}, Mohsen Zare^b, Ehsan Azad-Farsani^c

^a Electrical Engineering Department, University of Jiroft, Jiroft, Iran

^b Electrical Engineering Department, Jahrom University, Jahrom, Iran

^c Electrical Engineering Department, Golpayegan University of Technology, Golpayegan, Iran

ARTICLE INFO

Keywords:

Microgrid energy management
Photovoltaic systems
PV inverters
Robust optimization

ABSTRACT

Effective energy management of microgrid is essential due to significant growth of renewable energy resources like photovoltaic (PV) systems. Reactive power compensation capability provided by grid-tie PV inverters when PV power is unavailable increases the efficiency of the PVs utilization in microgrids. In this paper, a robust model combining particle swarm optimization (PSO) algorithm and primal–dual interior point (PDIP) method is proposed for optimal energy management of the microgrid, considering VAR compensation mode of the PV inverters. Besides, both the uncertainty of insolation forecast and forced outages of system components (diesel generators and branches) are taken into account. A bi-objective method is employed to detect the worst-case probable 24-h scenario with the severest effects on the system security. Finally, the energy management problem of the microgrid is solved under the obtained worst-case scenario, minimizing the microgrid operation cost, as well as satisfying the physical constraints of the microgrid and insolation limitation of the PVs. Simulation studies have been carried out on a modified version of IEEE 33-bus standard distribution system operating as a microgrid with variable PV generation. The results demonstrate the effectiveness of the proposed robust model for the microgrid energy management.

1. Introduction

Various drawbacks of traditional centralized power plants such as the high prices of fuels, environmental issues, low efficiency, high expenses of transmission network development, and the growing demand for the electricity have recently provided a number of challenges in the power systems. To address these issues, distributed energy resources (DER) have recently drawn much attention [1,2]. Microgrids are introduced to facilitate the integration of DERs into the power system. Microgrid is a small distribution system with local DERs which is connected to the traditional centralized electrical grid but is able to operate autonomously. A microgrid could be a kind of smart grid equipped with the advanced computer communication technologies and smart meters providing more flexibility and reliability for control and protection of the system. The microgrid operator optimizes the provided energy by the local DERs and the traditional centralized generation to supply the local loads. Interaction between DERs and the system infrastructure is the major feather of a microgrid. This interaction provides storage and flexibility abilities needed for demand management [3]. Photovoltaic (PV) system is one of the most effective DERs

in microgrids. Local generation and reducing the congestion rate of the transmission networks are the main advantages of the PVs. However the uncertainty of the solar irradiation availability of grid-tie PVs may provide some problems in active and reactive power balance and voltage regulation in microgrids [4].

Optimal dispatches of renewable energy resources (RESs) have been addressed in several works [5–13]. In [5], two sub-problems of distribution network reconfiguration and distribution system operation are integrated considering the uncertainties associated with wind, PV and load variation. In [9], a multi-objective optimization formulation incorporating both of the design problem and the optimal operation of distribution system is presented. In [13], a generalized model is proposed for distribution system optimal planning considering three aspects of modern distribution networks. First, a probabilistic approach considering the hourly load profile is employed; second, it is assumed that the distribution system is able to operate with one or multiple microgrids operating in islanding mode; finally the penetration level of RESs is taken into account.

The challenges with the grid-tie PV systems have been addressed in several studies. The impacts of utility-scale PV units on dynamic

* Corresponding author.

E-mail address: imangoroohi@ujiroft.ac.ir (I. Goroohi Sardou).

Nomenclature

Abbreviations

ASG	Adaptive scenario generation
BDSG	bi-objective desired solution generator
BOP	bi-objective problems
BLI	branches loading index
CSI	Current source inverter
DIG	Diesel generator
DER	distributed energy resource
FOR	forced outage rate
MOP	multi-objective optimization problem
MCS	Monte Carlo simulation
MOC	microgrid operation cost
MIPS	Matlab Interior Point Solver
NLP	nonlinear programming
PV	photovoltaic
PSO	particle swarm optimization
PDIP	primal-dual interior point
PF	power factor
PDF	probability density function
SCADA	supervisory control and data acquisition
RES	renewable energy resource
RPCF	reactive power compensation function
RWM	roulette wheel mechanism
VD	voltages deviations from the reference bus
VSI	Voltage source inverter
VOLL	the value of lost load
WCSD	worst-case scenario detection

Indices

<i>c</i>	system components (Diesel generators or branches)
<i>d</i>	diesel generators and PVs
<i>e</i>	objective functions
<i>g</i>	diesel generators (DIGs)
<i>h</i>	equal arc-shaped parts of angle θ
<i>i, j</i>	system buses
<i>it</i>	PSO iterations
<i>k</i>	types of system loads
<i>n</i>	non-contingent scenario
<i>p</i>	PVs at each bus
<i>s</i>	scenarios
<i>t, τ</i>	operation hours
<i>u</i>	insolation states
<i>w</i>	worst-case scenario

Parameters

FOR_c	forced outage rate of system components
I^{MPP}	current at maximum power point for the PVs (A)
I^{OC}	open-circuit current for the PVs (A)
Ins_u	insolation level obtained by the rotate wheel mechanism (KW/m ²)
K^I, K^V	current and voltage temperature coefficients for the PVs (A/°C and V/°C)
$LNS_i^{P,max}$	maximum active load shedding (KW)
N_B	total number of buses
N_S	total number of final most probable 24-h scenarios employed in robust and stochastic models
N_{SC}	total number of generated 24-h scenarios employed in the MCVM method

NPV_i	total number of PVs at each bus
$NDIG_i$	total number of DIGs at each bus
N_k	total number of load types
N_T	total number of operation hours
N^{md}	total number of PV modules
N_{ins}	total number of insolation levels
N_{com}	total number of system components (DIGs and branches)
$PPV_{p,i,t,s}^{av}$	available output power of PVs obtained by the insolation modelling (KW)
$PD_{i,t}$	active power demand (KW)
$PSUB_{i,t}^{max}$	feeder capacity (KW)
$PDIG_{g,i}^{min}$	lower limit for active power output of DIGs (KW)
$PDIG_{g,i}^{max}$	upper limit for active power output of DIGs (KW)
$PDER_d$	active power output of DIGs and PVs (KW)
$QD_{i,t}$	reactive power demand (KW)
$QDER_d$	reactive power output of DIGs and PVs (KVAR)
R_{DG}	DG penetration rate
S_{ij}^{max}	capacity of lines (MVA)
$SR_{g,i}^{max}$	upper limit for spinning reserves provided by DIGs (KW)
SR^{req}	total required spinning reserve of the microgrid at each hour
$S_{PDER_d}^{MOC}$	sensitivity of microgrid operation cost to deviation in the active power generation dispatch of DER <i>d</i>
$S_{PDER_d}^{VD}$	sensitivity of voltage deviation index to deviation in the active power generation dispatch of DER <i>d</i>
$S_{PDER_d}^{BLI}$	sensitivity of branches loading index to deviation in the active power generation dispatch of DER <i>d</i>
$S_{QDER_d}^{MOC}$	sensitivity of microgrid operation cost to deviation in the reactive power generation dispatch of DER <i>d</i>
$S_{QDER_d}^{VD}$	sensitivity of voltage deviation index to deviation in the reactive power generation dispatch of DER <i>d</i>
$S_{QDER_d}^{BLI}$	sensitivity of branches loading index to deviation in the reactive power generation dispatch of DER <i>d</i>
T^{cell}, T^{amb}	PV cell and ambient temperatures (°C)
T^{nom}	nominal operating temperature of PV cell (°C)
$URR_{g,i}$	up-ramp rates of DIGs
$DRR_{g,i}$	down-ramp rates of DIGs
$VOLL$	value of lost load (\$/KWh)
V_i^{ref}	reference value of the voltage (1 p.u)
V_i^{min}	minimum voltage magnitude (V)
V_i^{max}	maximum voltage magnitude (V)
V^{MPP}	voltage at maximum power point for the PVs (V)
V^{OC}	open-circuit voltage for the PVs (V)
w_e	weighting coefficient of the objectives
$Y_{ij,s}$	magnitude of admittance matrix elements (Ω)
$Z_{c,\tau,s}$	a binary variable which is equal to 0 if component <i>c</i> has been out of service for more than one hour at time τ ; otherwise it is equal to 1
$\alpha_{k,i}$	load importance factor
$\gamma_{u,\tau}^{ins}$	probability of <i>u</i> th insolation level
$\rho_{PSUB_{i,t}}$	cost of active power of substation (\$/KWh)
$\rho_{PV_{p,i,t}}$	operation and maintenance (O&M) cost of PV (\$/KWh)
$\rho_{DIG_{g,i,t}}$	O&M cost of DIG (\$/KWh)
ρ_{loss_t}	cost of active power losses (\$/KWh)
$\rho_{QSUB_{i,t}}$	cost of reactive power of substation (\$/KVARh)
$\rho_{g,i,t}^{SR}$	cost of spinning reserve of DIG (\$/KWh)
$\theta_{ij,s}$	angle of admittance matrix elements (rad)
β_s^0	type of scenario (1: non-contingent scenario, 0: contingent scenario)
$\pi_{t,s}$	probability of <i>s</i> th scenario up to time <i>t</i>
$\omega_{u,\tau,s}^{ins}$	binary indicators representing whether <i>u</i> th insolation level occurs (equal to 1) or not (equal to 0)
$\omega_{c,\tau,s}$	binary indicators representing the status of <i>c</i> th component (1: available, 0: forced outage)

$\lambda_{c,\tau,s}$	share of c th component in $\pi_{t,s}$	$PF_{p,i,t}^{PV}$	power factor of PVs
Variables		$PF_{p,i,t}^{DIG}$	power factor of DIGs
<i>ABLI</i>	average branches loading index	$Ploss_{\tau,s}$	hourly value of active power loss (KW)
<i>AENS</i>	average energy not supplied	$QSUB_{i,t,s}$	reactive power of substation (KVAR)
<i>AVD</i>	average sum of the buses voltage deviation from the reference bus	$QSUB_{i,t}^0$	scheduled value of reactive power of substation (KVAR)
<i>BLI_s</i>	branches loading index	$QPV_{p,i,t,s}$	reactive power output of PVs at each bus (KVAR)
$F_c(x)$	objective value	$QPV_{p,i,t}^0$	scheduled value of reactive power output of PVs at each bus (KVAR)
$F_c^{\min}(x)$	minimum value of the objective functions	$QDIG_{g,i,t,s}$	reactive power output of DIGs at each bus (KVAR)
$F_c^{\max}(x)$	maximum value of the objective functions	$QDIG_{g,i,t}^0$	scheduled value of reactive power output of DIGs at each bus (KVAR)
$LNS_{k,i,t,s}^P$	active load curtailment of different types (KW)	$S_{ij,t,s}$	apparent power flow of lines (MVA)
$LNS_{k,i,t,s}^Q$	reactive load curtailment of different types (KW)	$SR_{g,i,t}$	spinning reserve of DIGs at each bus (KW)
<i>MOC</i>	total operation cost of microgrid	$SR_{g,i,t}^0$	scheduled value of spinning reserve of DIGs at each bus (KW)
<i>MOC_n</i>	operation cost of microgrid under non-contingent scenario	$V_{i,t,s}$	voltage magnitude (V)
<i>MOC_w</i>	operation cost of microgrid under worst-case scenario	VD_s	sum of buses voltage deviation from the reference bus
$PSUB_{i,t,s}$	active power of substation (KW)	X^{1stg}	vector of first stage decision variables obtained by the PSO algorithm
$PSUB_{i,t}^0$	scheduled value of active power of substation (KW)	X^{2stg}	vector of second stage decision variables obtained by the PDIP method
$PPV_{p,i,t,s}$	active power output of PVs at each bus (KW)	$\delta_{ij,t,s}$	voltage angle (rad)
$PPV_{p,i,t}^0$	scheduled value of active power output of PVs at each bus (KW)	$\mu_c(x)$	normalized values of the objectives
$PDIG_{g,i,t,s}$	active power output of DIGs at each bus (KW)	μ	total normalized value
$PDIG_{g,i,t}^0$	scheduled value of active power output of DIGs at each bus (KW)		

(transient and small-signal stability) and static (voltage stability) of the transmission system are investigated in [14] and [15], including model of the PV array and converter, as well as associated control systems. Buses voltages limits are controlled by changing feed-in reactive power from the utility-scale PV units. A power factor control is employed to procure the reactive power set point. A voltage and frequency control is proposed in [15], coordinating the controls for the PV inverter and maximum power point tracking. In [4], the uncertainty in solar generation is stochastically modeled in the optimal operation of distribution network. Modeling of realistic PV generation in the proposed stochastic formulation improves the cost of power provision and minimizes the thermal loss. In [16], a probabilistic multi-objective method is presented for the operation of distribution networks improving the system voltage and power factor control. The uncertainties associated with solar irradiance of PVs and unbalanced loads are modeled. In [17], a systematic model is proposed for optimal dispatch of PV inverters in distribution feeders focusing on both active and reactive power production; the optimal PV inverters dispatch are determined for the ancillary services provision. The effect of PV penetration on the distribution system voltage profile is evaluated in [18]. In [19], a multi-objective model is presented for PV allocation in distribution system minimizing the power loss and improving the voltage profile. Time-varying loads are modeled to determine the PV penetration level in the distribution system. Ref. [20] presents a voltage unbalance sensitivity analysis to determine the optimal number and the size of single-phase PV systems in distribution network with multiple PV penetration levels. To this end, a stochastic method is proposed to verify the effectiveness of any random combination of PV systems in the network.

Solar irradiation and thereby PV active power generation are usually available during the middle hours of the day; so the PV inverters are useless and with no financial benefits during a large part of the 24 h period. This available inverter capacity can be utilized to produce reactive power for power loss reduction and voltage regulation during hours with low solar irradiation [1]. This capability to control the reactive power provides several ancillary services such as congestion management, power losses reduction and power/voltage control [21].

Microgrid energy management problem has been addressed in

several works [22–26]. In [22], a multi-objective framework is proposed for optimal energy management of the grid-tied microgrid considering wind speed forecast. Wavelet neural network is employed to improve the accuracy of the wind power forecast. In this work, economic dispatch based NSGA-II is used to solve the proposed multi-objective optimization problem (MOP). A new microgrid energy management scheme with the objectives of microgrid operation cost minimization and pollutant emission minimization is presented in [23]. The balance of charging/discharging amounts of energy storage systems over a day is considered by an interactive process. Besides, a graph is employed to observe the limits of the charge state. In this paper, multi-objective uniform water cycle algorithm is proposed to solve the proposed MOP. In [24], the microgrid energy management problem is solved minimizing the operation cost and carbon emissions. Besides, the disturbances of intermittent renewable energy resources and uncertain loads are mitigated. Multi-objective cross entropy algorithm is employed to solve the proposed MOP. The problem of optimal sizing of battery storage is combined with the problem of optimal economic dispatches of the microgrid resources in [25]. The proposed model considers the daily price profile of the electricity and natural gas, limits of battery state of charge and the non-linearity of the PV output power. In [26], the benefits of coupling of a storage system with a RES and a complex of electrical loads in a microgrid, is verified by a sensitivity analysis, from both economic and energy point of views. In this work, the interactions among the different microgrid subsections are considered on a yearly base. Ref. [27] presents an evolutionary technique named improved bat algorithm to procure an optimized operation management of the microgrid in the presence of battery energy storage sizing.

In several works such as [10,13,19] the weighted sum approach is employed to solve the proposed MOPs. This method obtains a set of Pareto solutions by varying the weights of multiple objectives. However, this method cannot provide the Pareto solutions for the problems with non-convex fronts, which reduces its applicability. ϵ -constraint method is used to solve the MOP proposed in [16]. This method determines the Pareto solutions by converting the problem into a parameter-dependent scalar optimization problem. Several solutions of the MOPs are obtained by solving the scalar problem for a variety of

parameters. The main disadvantage of this method is high computation burden due to the necessity to approximate the Pareto front. In some other works such as [7,9,11,22–24], a set of non-dominated solutions of MOPs are procured by meta-heuristic based approaches like NSGA-II, MOUWCA, MOCE and MOPSO. Although these approaches remedy the above drawbacks, there is no guarantee that the obtained set of non-dominated solutions is a good approximate of the real Pareto front. Furthermore, for all of the above methods, a decision making approach, as in [10], is needed to find the best compromise solution among the approximated Pareto front set.

In the above studies on the microgrid energy management, the uncertainties are not incorporated in the problem formulation. However, a scenario-based programming model is essential to decrease the risk of renewable energy intermittency and uncertainty, as well as unsuccessful commitment of generators. In [28], a scenario-based stochastic programming model is proposed for optimal energy management of the microgrid minimizing the cost and emission. The uncertainties of load forecast, wind and photovoltaic available energy, as well as the market price are taken into account. However, in scenario-based stochastic approaches the system uncertainties are modeled by considering a large number of possible scenarios which may lead to large-sized, computationally challenging problems. Besides, the probabilistic functional (e.g. expected value) of the objective functions and constraints are considered in the stochastic optimization problem. Share of each scenario in the expected values of the objectives is computed with respect to the normalized value of that scenario probability. This does not guarantee the optimal optimization of the objective functions in the mathematical optimization scenario-based problem. Moreover, although the most probable scenarios are considered in the stochastic model, there is no guarantee that a contingency out of the considered scenarios does not occur. Consequently, it is essential to make the system robust enough to withstand probable contingencies out of the considered scenarios. Furthermore, both wait and see, and here and now stochastic problems require representation of uncertainties in the probabilistic space and then the propagation of these uncertainties through the model to achieve the probabilistic representation of the output [29]. This provides a new challenge for the microgrid operator to aggregate the scenarios to obtain the final values for the scenario dependent variables. For example in [30], weighted-average (expected value) of the variables over all scenarios are applied. To remedy this weakness, a robust optimization model is proposed in the present paper for optimal energy management of the microgrid aiming at operation cost minimization. The energy management problem of the microgrid is solved under worst-case scenario making the system robust enough to withstand probable contingencies. The hybrid particle swarm optimization (PSO) algorithm and primal-dual interior point (PDIP) method is employed to solve the proposed microgrid energy management problem. To this end, the nonlinear programming (NLP) problem of the microgrid energy management is solved by the PDIP method, while the dispatches of the reserves resources and optimal power factors (PFs) of DERs are determined as the particles' positions in the PSO algorithm. In the hybrid method, the dispatches of the reserves resources and optimal PFs of DERs, which are defined as scenario independent variables (first stage decision variables) obtained by the PSO algorithm, act as constant parameters in the NLP problem solved by the PDIP method. This reduces the complexity and non-linearity of the problem in compared to the traditional methods in which all the decision variables are obtained as scenario dependent variables (second stage decision variables). Besides, the need for a scenario aggregation approach to obtain the final values of these variables (the dispatches of the reserves resources and optimal PFs of DERs) is eliminated. Furthermore, bi-objective desired solution generator (BDSG) approach which is presented in our other work, is employed to solve the bi-objective problems (BOPs) for detecting the worst-case probable scenario, maximizing the security indices of buses voltages deviations from the reference bus (VD) and branches loading index

(BLI) [31]. BDSG approach is able to achieve the desired solution for both convex and non-convex BOPs, without acquiring the complete Pareto front through approximation. The main contributions of this paper with respect to the previous works can be summarized as: (1) combining the advantages of both classic and heuristic methods to facilitate applying the PDIP method to the microgrid energy management problem, (2) considering VAR compensation mode of grid-tie PV inverters to optimize the 24-h utilization of PVs in the microgrid energy management, (3) proposing a bi-objective approach for detecting the worst-case probable scenario among the 24-h generated scenarios, and (4) proposing a validation method based on Monte Carlo simulation, which is referred to as MCVM method, to evaluate the performance and potential of the proposed robust model versus the traditional stochastic one.

The rest of the paper is organized as follows: Section 2 describes the formulation for the robust energy management of the microgrid with PV inverters. The employed robust model is detailed in Section 3. Besides, the proposed MCVM validation method is presented in this section. Section 4 presents a case study to verify the efficiency of the proposed method, and Section 5 presents the conclusion.

2. Problem formulation

In order to focus on the underlying ideas of the optimal utilization of grid-tie PV inverters, and for the sake of simplicity, it is assumed that the microgrid includes just photovoltaic and diesel generator (DIG) DERs and other types of DERs are ignored. In this section, first the model of the PV generation is presented. Then, the proposed robust model for optimal energy management of the microgrid is presented. At the end, the proposed MCVM validation method is described.

2.1. PV generation model

In grid-tie PV systems, the output direct currents (DC) of the solar modules are converted to the alternate current (AC) by an inverter. Current source inverters (CSI) are able to supply only active power (operating at $PF = 1$). Consequently, when the solar irradiation is low especially during the night, such PV systems become idle and are incapable of feeding the grid loads [32]. Voltage source inverter (VSI) has recently received increasingly interest. In contrast to the CSI, VSI has the capability to inject and absorb reactive power to the electric grid according to the grid demand. This capability provides a new function which is referred to as reactive power compensation function (RPCF). RPCF is effective when the insolation is weak or during the night. By this function the inverters are able to absorb as little as possible active power from the grid, set their DC bus voltages within limits, and inject the desired reactive power into the grid. Microgrid energy management is improved economically and technically by RPCF. Power factor of the PV system is set based on the supplied energy by the PV system varying with the solar irradiation level. On the basis of microgrid operation requirements, the direction of the voltage vector may be changed, so that the inverter is absorbing reactive power from the grid [33].

In this paper, historical data are employed to generate a forecasting model for the insolation at each hour. Accurate forecast of insolation, leads to a more accurate energy management of the microgrid. To increase the reliability of the prediction, dependable levels of the insolation forecast are extracted. To this end, a probability density function (PDF) is generated for the insolation at each hour. As shown in Fig. 1, the PDF of the insolation is separated into seven states with one insolation forecast error standard deviation (σ) wide which are centered on the zero mean. Here, the roulette wheel mechanism (RWM) is employed to generate scenarios for each hour. To this end, probabilities of different insolation states obtained from the respective PDF are normalized such that range of [0,1] is occupied by the normalized probabilities, and their summation becomes equal to unity. Then, random numbers are generated between 0 and 1, where each random number

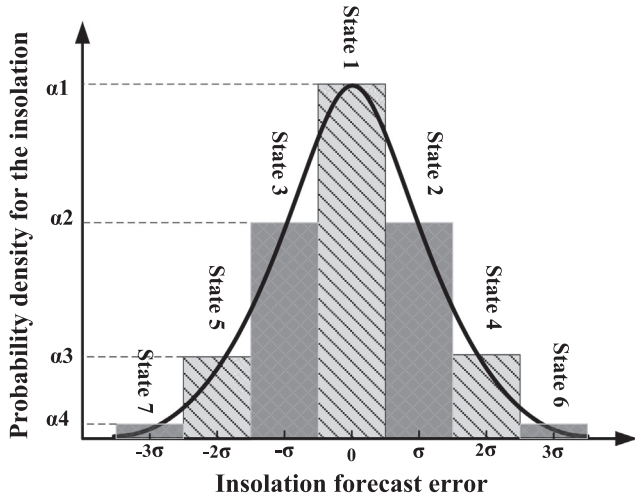


Fig. 1. Discretization of the probability distribution of the insolation forecast.

falls in the normalized probability range associated with an insolation level. That insolation level is selected by the RWM for the corresponding scenario [28].

Based on the insolation level obtained by the RWM (Ins_u), the available output power of the PV module for each insolation state (PPV_u^{av}) is calculated by (1). T^{cell} in (1) denotes cell temperature and is obtained by (2) [19].

$$PPV_u^{av} = N^{md} \left(\frac{V^{MPP} I^{MPP}}{V^{OC} I^{SC}} \right) (V^{OC} - K^V T^{cell}) Ins_u (I^{SC} + K^I (T^{cell} - 25)) \quad (1)$$

$$T^{cell} = T^{amb} + Ins_u \left(\frac{T^{nom} - 20}{0.8} \right) \quad (2)$$

2.2. Uncertainties modelling

In addition to the insolation forecast uncertainty, the uncertainties regarding the contingencies of system components (DIGs and branches) are modeled by Monte Carlo simulation (MCS) based on their forced outage rates (FORs) [30]. To this end, in each scenario of the MCS, a number between [0,1] is randomly generated for each component, and compared with its FOR. If the number generated for a component is smaller than its FOR, then the component is out of service; otherwise, it is available. This procedure is iterated for all DIGs and branches. The procured insolation level by the RWM, as well as the status of DIGs and branches determined by the MCS construct one scenario of the robust model for an hour. The process continues until a number of scenarios are generated for an hour. Adaptive scenario generation (ASG) algorithm as described in [30] is used in this paper to generate 24-h scenarios. In the proposed ASG algorithm, the probability of sth generated scenario up to hour t ($\pi_{t,s}$) can be computed by (3) and (4). As shown in (4), it is assumed that if a forced outage of a system component (DIG or branch) occurs in an hour, it lasts for a specific number of hours. Increasing the number of scenarios for the proposed robust model results in a better uncertainties modeling with the cost of higher computation burden. Consequently, a scenario reduction technique is used to reduce the number of generated scenarios while still retaining the essential features of the employed ASG algorithm [30]. Employing the reduction technique the most probable and dissimilar 24-h scenarios are extracted (N_s scenarios) for using in the proposed robust model.

$$\pi_{t,s} = \prod_{\tau=1}^t \left(\sum_{u=1}^{N_{ins}} \omega_{u,\tau,s}^{ins} \gamma_{u,\tau}^{ins} \cdot \prod_{c=1}^{N_{com}} \lambda_{c,\tau,s} \right) \quad (3)$$

$$\lambda_{c,\tau,s} = [(\omega_{c,\tau,s} (1 - FOR_c) + (1 - \omega_{c,\tau,s}) FOR_c)] Z_{c,\tau,s} + (1 - Z_{c,\tau,s}) \quad (4)$$

2.3. Robust energy management of the microgrid

In this paper, a robust optimization model is proposed for the microgrid energy management problem, in which the worst-case probable 24-h scenario is detected. The microgrid energy management problem is solved under the obtained worst-case scenario, making the system ‘robust’ enough to provide an adequate level of the network security. In other words, the microgrid is utilized to be capable of withstanding a major event with the severest effects on the system security. After detection of the worst-case scenario, the microgrid energy management problem is solved under this scenario, and the optimal dispatches of DERs are obtained. Optimizing the operational scheduling of the microgrid resources under the worst-case scenario in the proposed robust model provides more robust solutions with a relatively low computational burden in compared to the stochastic and probabilistic approaches. Besides, the optimality of the solutions is improved due to the optimization of the real values of the objectives instead of the expected values of the objectives. It is to be noted that two optimization problems are solved in the proposed robust model for energy management of the microgrid. First, the main problem of the microgrid energy management with objective of operation cost minimization, second, bi-objective worst-case scenario detection (WCSD) problem, maximizing the security indices of buses voltages deviations from the reference bus (VD) and branches loading index (BLI).

2.3.1. Main problem

The main problem of the microgrid energy management is formulated as a constrained nonlinear optimization problem. Non-contingent scenario with no insolation error ($\sigma = 0$) and component outage (normal operation state), as well as the worst-case scenario are considered in the proposed formulation, as follows:

Objective function: The objective is to minimize the total operation cost of the microgrid (MOC) which is sum of the operation costs under the non-contingent scenario (MOC_n) and the operation costs under worst-case probable 24-h scenario (MOC_w), as shown in (5). Operation costs include the cost of active and reactive power supplied by the substation (main grid), the operation cost of the DERs, and the cost of active power losses. Besides, as shown in (6) and (7), cost of reserves provided by DIGs is included in the non-contingent scenario, while the respective penalties associated with the unserved loads are included in the worst-case scenario. In fact, the costs of reserves deployment in the post contingency states are included in energy cost under relevant scenario. To prevent high penalty load curtailment, the priorities of individual loads are taken into account by defining load importance factors, which depend on the type and location of the loads [34].

$$\text{Min MOC} = MOC_n + MOC_w \quad (5)$$

$$MOC_n = \sum_{i=1}^{N_T} \left(P_{loss_{i,n}} \cdot \rho_{loss_i} + \sum_{i=1}^{N_B} \left(P_{SUB_{i,t,n}} \cdot \rho_{PSUB_{i,t}} + Q_{SUB_{i,t,n}} \cdot \rho_{QSUB_{i,t}} + \sum_{p=1}^{NPV_i} PPV_{p,i,t,n} \cdot \rho_{PV_{p,i,t}} + \sum_{g=1}^{NDIG_i} (PDIG_{g,i,t,n} \cdot \rho_{DIG_{g,i,t}} + SR_{g,i,t} \cdot \rho_{g,i,t}^{SR}) \right) \right) \quad (6)$$

$$MOC_w = \sum_{i=1}^{N_T} \left(P_{loss_{i,w}} \cdot \rho_{loss_i} + \sum_{i=1}^{N_B} \left(P_{SUB_{i,t,w}} \cdot \rho_{PSUB_{i,t}} + Q_{SUB_{i,t,w}} \cdot \rho_{QSUB_{i,t}} + \sum_{p=1}^{NPV_i} PPV_{p,i,t,w} \cdot \rho_{PV_{p,i,t}} + \sum_{g=1}^{NDIG_i} PDIG_{g,i,t,w} \cdot \rho_{DIG_{g,i,t}} + VOLL \cdot \sum_{k=1}^{N_K} \alpha_{k,i} \cdot LNS_{k,i,t,w}^p \right) \right) \quad (7)$$

Constraints: The problem of optimal energy management of the microgrid includes several practical constraints. The active power of substation is limited by the feeder capacity as shown in (8). Constraints (9) and (10) address the power flow equations, considering the active and reactive power output of DERs. As shown in (10), it is possible for PVs to absorb reactive power, depending on total reactive demand, reactive output of DIGs, and the reactive power supplied by the substation. Insolation limitation of PVs is addressed in (11). As shown in (11), available output power of each PV obtained by the insolation modelling ($PPV_{p,i,t,s}^{av}$) is considered as the upper limit for the active power output of that PV at each hour. The proposed formulation for the optimal energy management of the microgrid allows utilization of the RPCF available by the PVs. When the insolation is weak, a significant part of reactive power demand can be supplied by the PV inverters (as in (10)); this reduces the operation cost by decreasing the reactive power supplied by the substation (as in (5)–(7)). Spinning reserves provided by DIGs are limited by (12). Constraint (13) addresses the total required spinning reserve of the microgrid at each hour. As shown in (14) and (15), the power outputs of DIGs under non-contingent scenario are limited by the scheduled dispatches of the reserves resources; while under contingencies the power output deviations of the DIGs from the normal state values are limited by the scheduled dispatches of the reserves resources. In fact, energy and reserves are scheduled so that the system is remained secure under the contingent scenarios, while there is minimum deviation in power output of DIGs with respect to that of the non-contingent scenario. Response rate limitations of the DIGs are shown in (16) and (17). The load curtailment at each bus is restricted by (18). As shown in (19), no load curtailment is allowed under non-contingent scenario. Constraints (20) and (21) confine the power flow of the lines and the buses voltages, respectively.

$$PSUB_{i,t,s} \leq PSUB_{i,t}^{\max} \quad (8)$$

$$PSUB_{i,t,s} + \sum_{p=1}^{NPV_i} PPV_{p,i,t,s} + \sum_{g=1}^{NDIG_i} PDIG_{g,i,t,s} - (PD_{i,t} - \sum_{k=1}^{Nk} LNS_{k,i,t,s}^P) = \sum_{j=1}^{N_B} |V_{i,t,s}| |V_{j,t,s}| |Y_{ij,s}| \cos(\delta_{ij,t,s} - \theta_{ij,s}) \quad (9)$$

$$QSUB_{i,t,s} + \sum_{p=1}^{NPV_i} QPV_{p,i,t,s} + \sum_{g=1}^{NDIG_i} QDIG_{g,i,t,s} - \left(QD_{i,t} - \sum_{k=1}^{Nk} LNS_{k,i,t,s}^Q \right) = \sum_{j=1}^{N_B} |V_{i,t,s}| |V_{j,t,s}| |Y_{ij,s}| \sin(\delta_{ij,t,s} - \theta_{ij,s}) \quad (10)$$

$$PPV_{p,i,t,s} \leq PPV_{p,i,t,s}^{av} \quad (11)$$

$$SR_{g,i,t} \leq SR_{g,i}^{\max} \quad (12)$$

$$\sum_{g=1}^{NDIG_i} SR_{g,i,t} \geq SR^{req} \quad (13)$$

$$PDIG_{g,i}^{\min} \leq PDIG_{g,i,t,s} \leq PDIG_{g,i}^{\max} - SR_{g,i,t} \quad (14)$$

$$\max\{PDIG_{g,i}^{\min}, PDIG_{g,i,t,n}\} \leq PDIG_{g,i,t,s} \leq \min\{PDIG_{g,i}^{\max}, PDIG_{g,i,t,n} + SR_{g,i,t}\} \quad \forall s = \{1, \dots, N_S\}, s \neq n \quad (15)$$

$$PDIG_{g,i,t,s} - PDIG_{g,i,t-1,s} \leq URR_{g,i} \quad (16)$$

$$PDIG_{g,i,t-1,s} - PDIG_{g,i,t,s} \leq DRR_{g,i} \quad (17)$$

$$\sum_{k=1}^{Nk} LNS_{k,i,t,s}^P \leq LNS_{i,t}^{P,\max} \quad (18)$$

$$LNS_{k,i,t,n}^P = LNS_{k,i,t,n}^Q = 0 \quad (19)$$

$$S_{ij,t,s} \leq S_{ij}^{\max} \quad (20)$$

$$V_i^{\min} \leq V_{i,t,s} \leq V_i^{\max} \quad (21)$$

2.3.2. Worst-case scenario detection problem

To detect the worst-case scenario among N_S most probable generated 24-h scenarios, the microgrid energy management problem is solved under these scenarios with the objectives of maximization of the sum of buses voltages deviations from the reference bus (VD), and branches loading index (BLI), satisfying constraints (8)–(11), and (15)–(18). This problem is called worst-case scenario detection (WCSD) problem whose objectives are formulated in (22) and (23). Limits violation in the buses voltages and branches power flows are the main security concerns of the microgrid operator. That is why indices of VD and BLI are chosen as the objectives of the bi-objective WCSD problem. After solving the bi-objective WCSD problem under N_S generated most probable 24-h scenarios, scenario under which the WCSD problem leads to the solution with higher values of indices VD and BLI is chosen as the worst-case probable scenario. In fact, the scenario with the severest effects on the system security is detected.

$$Max \quad F_1 = VD_s = \sum_{t=1}^{N_T} \sum_{i=1}^{N_B} \frac{|V_{i,t,s} - V_i^{ref}|}{V_i^{ref}} \quad (22)$$

$$Max \quad F_2 = BLI_s = \sum_{t=1}^{N_T} \sum_{i=1}^{N_B} \sum_{\substack{j=1 \\ j \neq i}}^{N_B} \left(\frac{S_{ij,t,s}}{S_{ij}^{\max}} \right) \quad (23)$$

3. Solution methodology

The main difficulty with the MOPs including the conflicting objectives is lack of a solution that allows for simultaneous optimality of all objectives. Here, the BDSG approach which is proposed in our other work is employed to solve the proposed bi-objective WCSD problems [31]. Against the scalarization methods such as ϵ -constraint method, and metaheuristic methods such as NSGA-II and MOPSO, BDSG approach provides the desired solution without need to obtain an approximation of the Pareto front. This significantly reduces the computational burden, and removes the necessity of employing a decision making approach to find the best compromise solution among the Pareto solutions.

3.1. BDSG approach

In this approach, we are looking for a Pareto solution of bi-objective problem (BOP) shown in (24), which minimizes $|\mu_2(x) - m\mu_1(x)|$. Where, m is a positive real number which can be tuned based on the microgrid operator preference. For instance, $m = 1$ indicates second objective (BLI) is as important as the first objective (VD) ($w_1 = 1/2$, $w_2 = 1/2$). The objective functions are normalized by (25). The first step of BDSG approach is to solve Problem (26) with $a = 0$ and $r = (1, m)^T$, where “lexmin” means lexicographically minimizing the objective. It can be shown that obtained solution of Problem (26) which is denoted as x^0 is a Pareto solution of BOP (24) [31]. Three cases are possible for x^0 :

Case 1: $\mu_2(x^0) = m\mu_1(x^0)$: Here, x^0 is the desired solution, and the algorithm stops.

Case 2: $\mu_2(x^0) < m\mu_1(x^0)$: In this case, first, as shown in Fig. 2 for a typical BOP, parameter d^0 which denotes the distance between $\mu(x^0)$ and the line $\mu_2 = m\mu_1$ is computed. Then α and θ are calculated by (27) and (28). To investigate whether Pareto solution x^0 minimizes $|\mu_2(x) - m\mu_1(x)|$ over the Pareto frontier, the space \mathbb{R}^2 is divided into four regions with respect to the point $\mu(x^0)$, as shown in (29).

$$BOP: \min \mu(x) = (\mu_1(x), \mu_2(x)) \quad (24)$$

$$\mu_e(x) = \frac{F_e^{\max}(x) - F_e(x)}{F_e^{\max}(x) - F_e^{\min}(x)} \quad e = 1, 2 \quad (25)$$

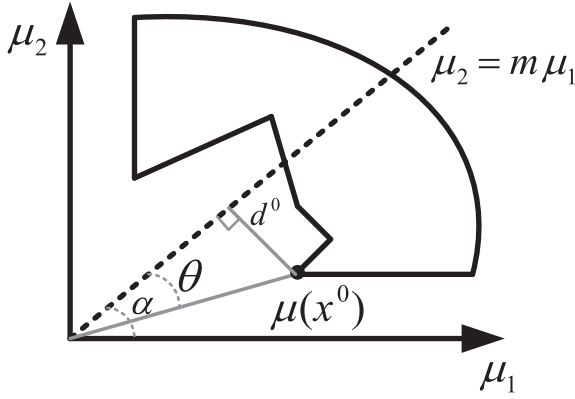


Fig. 2. Parameters α , θ and d^0 for the BDSG approach.

$$\theta = \arcsin\left(\frac{d^0}{\sqrt{(\mu_1(x^0))^2 + (\mu_2(x^0))^2}}\right) \quad (28)$$

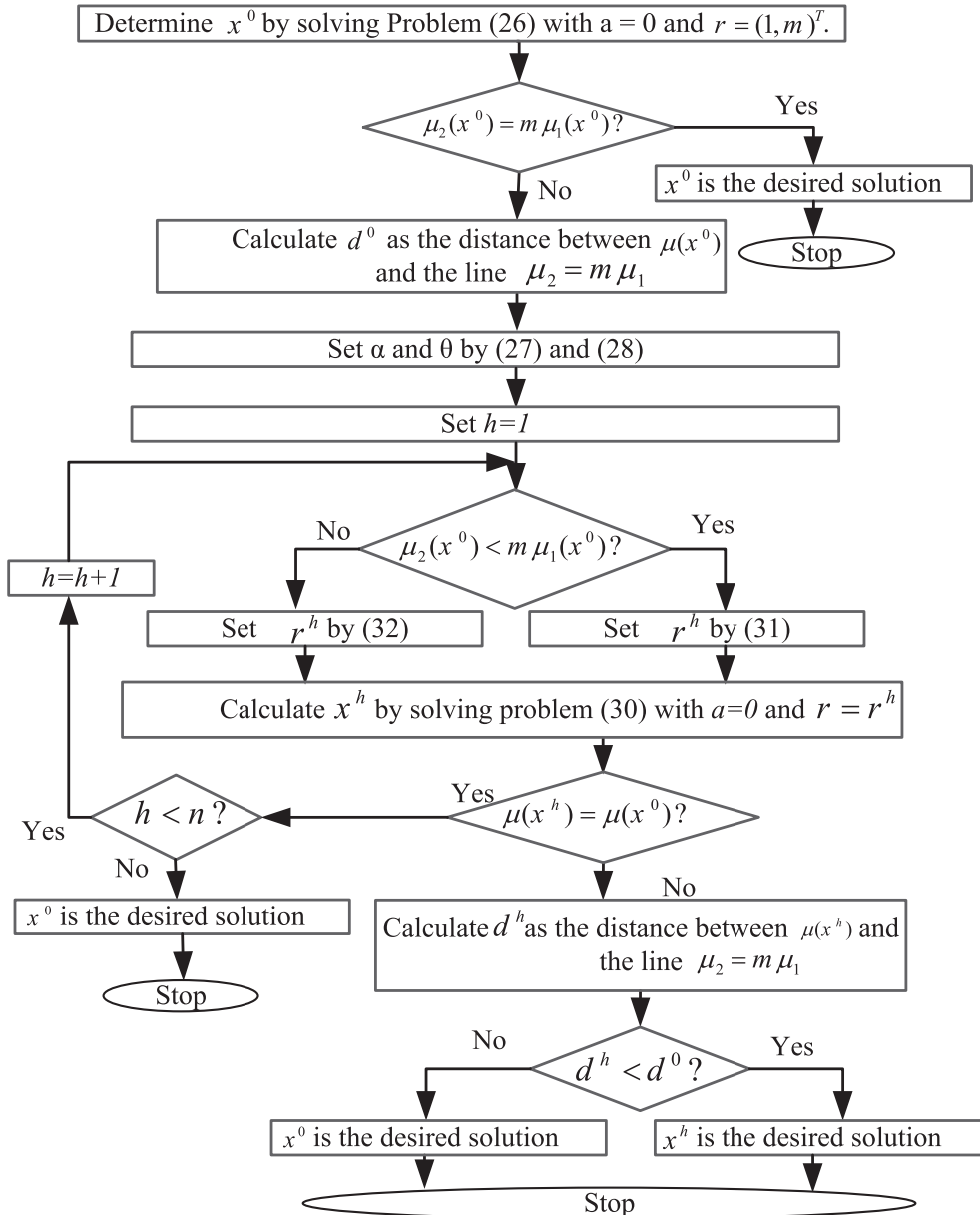
$$R_1 := \{(y_1, y_2) \in R^2 | y_1 \geq \mu_1(x^0), y_2 \geq \mu_2(x^0)\} R_2 := \{(y_1, y_2) \in R^2 | y_1 < \mu_1(x^0), y_2 > \mu_2(x^0)\} R_3 := \{(y_1, y_2) \in R^2 | y_1 \leq \mu_1(x^0), y_2 \leq \mu_2(x^0)\} R_4 := \{(y_1, y_2) \in R^2 | y_1 > \mu_1(x^0), y_2 < \mu_2(x^0)\} \quad (29)$$

Let \bar{x} be a Pareto solution such that $\mu(\bar{x}) \neq \mu(x^0)$. If $\mu(\bar{x}) \in R_1$, then it is dominated by x^0 ; so it is not possible for \bar{x} to be a Pareto solution. Besides, if $\mu(\bar{x}) \in R_3$, then it dominates x^0 ; so it is not possible for x^0 to be a Pareto solution. Consequently, $\mu(\bar{x})$ is located in one of regions R_2 or R_4 . If $\mu(\bar{x}) \in R_4$, then the distance between $\mu(x^0)$ and the line $\mu_2 = m\mu_1$ is less than the distance between $\mu(\bar{x})$ and the line $\mu_2 = m\mu_1$. Therefore, $\mu(\bar{x}) \in R_2$, and the search space is confined to region R_2 . Now, we are looking for Pareto solution \bar{x} located in region R_2 minimizing $|\mu_2(x) - m\mu_1(x)|$. As the Pareto solutions located in R_2 , are not dominated by points located in region $R_1 \cup R_4$, the constraint $\mu_1(x) \leq \mu_1(x^0)$ is added to the Problem (26), and Problem (30) is solved to obtain all Pareto solutions in which the distance between their image

$$\text{lexmin}(t, \mu_1(x) + \mu_2(x)) \text{ s. t. } a + tr - \mu(x) \geq 0 \quad (26)$$

$$\alpha = \arctan(m) \quad (27)$$

Fig. 3. The algorithm of the proposed BDSG approach.



and the line $\mu_2 = m\mu_1$ is less than the distance between $\mu(x^0)$ and the line $\mu_2 = m\mu_1$. In (30), $a = 0$ and r^h is calculated by (31). Parameter n in (31) is a given fixed positive integer and denotes the number of choices for the parameter r^h . Larger value of n leads to a better approximation of the desired solution.

$$\text{lexmin}(t, \mu_1(x) + \mu_2(x)) \text{ s. t. } a + tr^h - \mu(x) \geq 0, \mu_1(x) \leq \mu_1(x^0) \quad (30)$$

$$r^h = \sqrt{1 + m^2} \left(\cos\left(\alpha + h\frac{\theta}{n}\right), \sin\left(\alpha + h\frac{\theta}{n}\right) \right), \quad h = 1, 2, \dots, n \quad (31)$$

Let (t^h, x^h) be the optimal solution of Problem (30) in h th iteration. If $\mu(x^h) = \mu(x^0)$, we go to the next iteration ($h = h + 1$); otherwise, the distance between $\mu(x^h)$ and the line $\mu_2 = m\mu_1$, which is denoted as d^h , is computed. If $d^h < d^0$, then x^h is the desired solution; otherwise x^0 is the desired solution. It is to be noted that, after procuring the first x^h with $\mu(x^h) \neq \mu(x^0)$, the next iteration is not necessary. This is due to increasing the value of d^h by increasing the value of h .

Case 3: $\mu_2(x^0) > m\mu_1(x^0)$: An approach similar to Case 2 is taken for Case 3, except that (31) is replaced by (32).

$$r^h = \sqrt{1 + m^2} \left(\cos\left(\alpha - h\frac{\theta}{n}\right), \sin\left(\alpha - h\frac{\theta}{n}\right) \right) \quad (32)$$

The above steps are summarized in the algorithm of the BDSG approach shown in Fig. 3.

3.2. Solution algorithm

Employing the BDSG approach for the BOP WSCD problems, several single-objective sub-problems (as shown in (26) and (32)) are obtained which should be solved. Hybrid PSO algorithm and PDIP method is employed to solve all NLP problems including the main energy management problem of the microgrid and the sub-problems obtained by the BDSG approach [7,35]. The connection of PSO algorithm, PDIP method and BDSG approach for robust energy management of the microgrid is shown in Fig. 4. Interior point method is able to obtain approximate solutions of nonlinear-hard problems in polynomial time. In interior point methods, the expensive operations can somewhat be parallelized; consequently, they can better exploit multiprocessor platforms; thereby tend to be faster on large problems [35]. Because of this and due to the complexity of the proposed problem of optimal hourly operation of the microgrid including the PVs, PDIP method is employed to solve the NLP problems; this is while the first stage scenario-independent decision variables including the optimal dispatches of the reserves resources, and PFs of DERs are determined as the particles' positions in the PSO algorithm. In fact, for a given particles' position (first stage decision variables) a subsidiary NLP problem is solved using PDIP method in each iteration of the PSO algorithm to obtain optimal hourly dispatches of the microgrid resources.

Fig. 5 shows the solution algorithm of the proposed robust model for microgrid energy management. Steps (a)-(p) in this figure are the main steps taken to obtain the proposed microgrid energy management scheme which are described as follows:

- (a) Receive input data including hourly insolation data, load data, forced outage rates (FORs) of the microgrid elements, and marginal costs.
- (b) Employ roulette wheel mechanism and Monte Carlo simulation to generate N_S most probable 24-h scenarios as detailed in Sections 2.1 and 2.2.
- (c) Select randomly the initial population of particles' positions, and velocity vectors in the PSO algorithm. Here, particles' positions represent the first stage decision variables, including reserves dispatches of DIGs, and PFs of DERs as shown in (33).

$$X^{1stg} = [PF_{p,i,t}^{PV}, PF_{g,i,t}^{DIG}, SR_{g,i,t}] \quad (33)$$

- (d) The search space boundaries are validated for particles' positions. In iteration 2 and higher ($it \geq 2$), updating the particles' positions by the PSO operators may violate the variable bounds. If so, go to (e), otherwise go to (f).
 - (e) Move the infeasible solution to the closest random feasible solution.
 - (f) Based on reserves dispatches of DIGs obtained in Step (c), the PDIP method is employed to solve the main energy management problem of the microgrid under the non-contingent scenario, minimizing MOC_n shown in (6), and satisfying constraints shown in (8)–(14), (16), (17), and (19)–(21). Here, the active power output of the PVs, as well as the active and reactive power of the substation are the second stage decision variables as shown in (34); while the reactive power outputs of PVs and DIGs are computed as shown in (35) and (36), respectively.
- $$X^{2stg} = [PPV_{p,i,t,s}, PDIG_{g,i,t,s}, PSUB_{i,t,s}, QSUB_{i,t,s}] \quad (34)$$
- $$QP_{p,i,t,s} = PPV_{p,i,t,s} \tan(\cos^{-1}(PF_{p,i,t}^{PV})) \quad (35)$$
- $$QDIG_{p,i,t,s} = PDIG_{p,i,t,s} \tan(\cos^{-1}(PF_{p,i,t}^{DIG})) \quad (36)$$
- where, $PF_{p,i,t}^{PV}$ and $PF_{p,i,t}^{DIG}$ are also determined as the particles' position of the PSO algorithm.
- (g) Solve the single-objective WSCD problems under the generated probable 24-h scenarios, with objectives (22) and (23), and constraints shown in (8)–(11), and (15)–(18), separately, to obtain the boundaries of the objectives.
 - (h) Based on the dispatches schedule of the resources under the non-contingent scenario obtained in Step (f), the BDSG approach (as

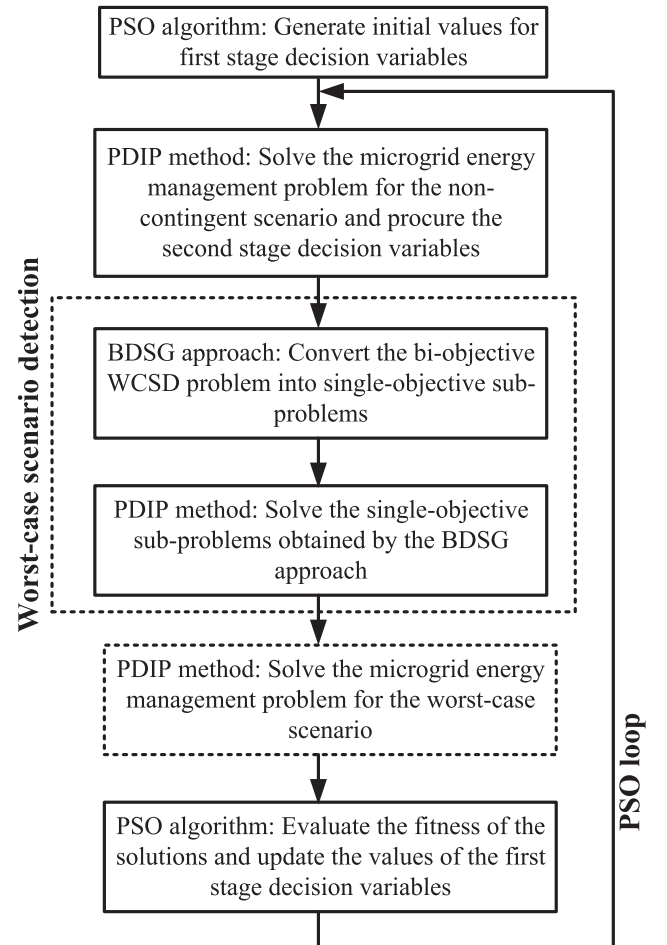


Fig. 4. Connection of different methods for robust energy management of the microgrid.

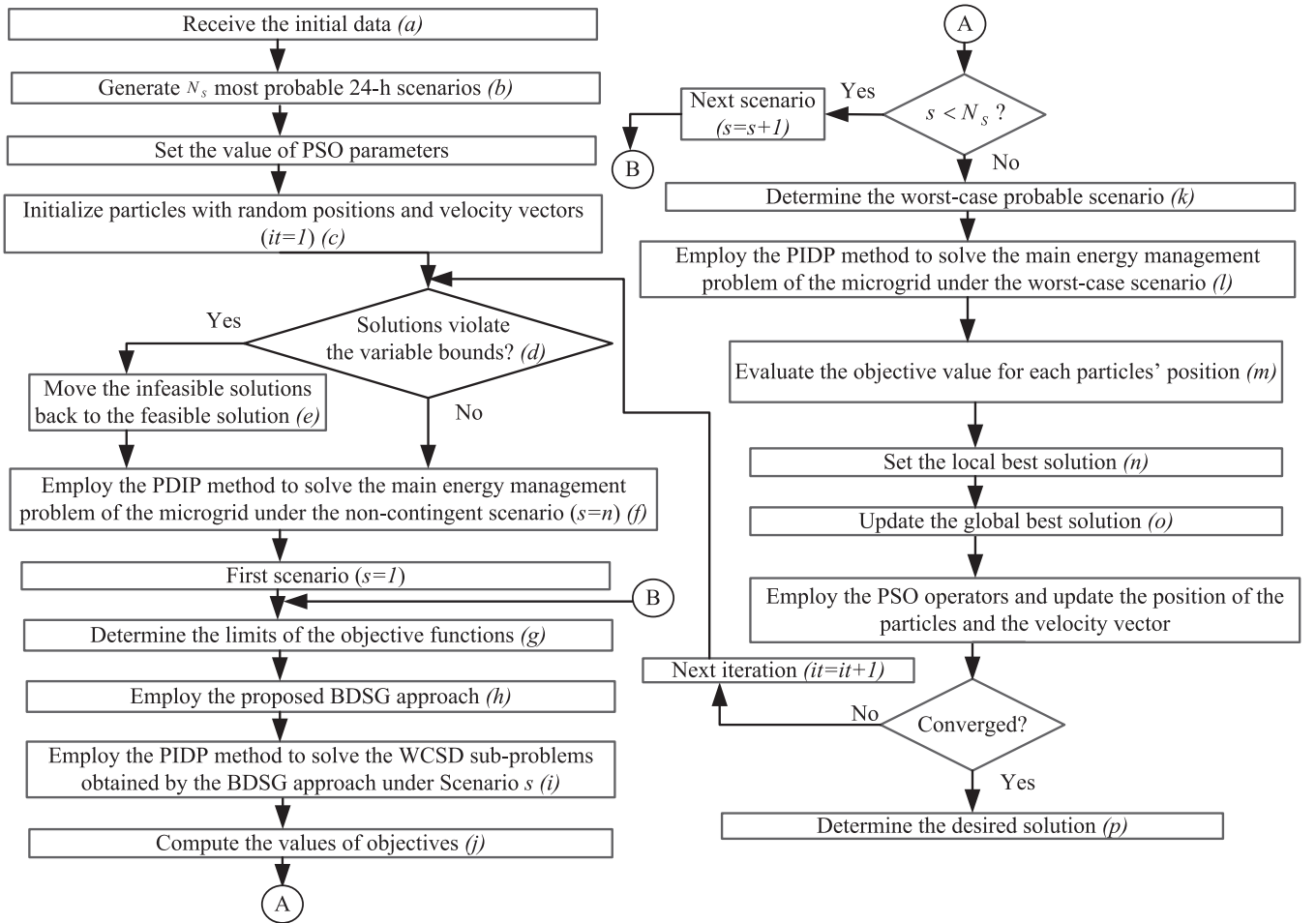


Fig. 5. The proposed algorithm for robust energy management of the microgrid with PV inverters.

detailed in Section 3.1) is applied to solve the BOP WCSD problem under the generated scenarios, maximizing objectives (22) and (23), and satisfying constraints shown in (8)–(11), and (15)–(18). Here, the load curtailments are considered equal to zero ($LNS_{k,i,t,s}^p = LNS_{k,i,t,s}^o = 0$).

- (i) Employ the PDIP method to solve the single-objective WCSD sub-problems obtained by the BDSG approach.
- (j) Calculate the values of first objective function (VD) shown in (22) and the second objective function (BLI) shown in (23) based on the optimal dispatches of microgrid resources procured in Steps (f) and (i).
- (k) After solving the BOP WCSD problems for all N_s probable 24-h scenarios by the BDSG approach, the scenario with smallest value of μ (as calculated in (37)) is chosen as the worst-case scenario.

$$\mu = w_1\mu_1 + w_2\mu_2 \quad (37)$$

where, w_1 and w_2 denote the weighting coefficients of the objectives and are set based on the microgrid operator preference ($w_1 = 1/(1 + m)$, $w_2 = m/(1 + m)$).

- (l) Based on the dispatches schedule of the resources under the non-contingent scenario obtained in Step (f), the PDIP method is employed to solve the main energy management problem of the microgrid under the worst-case probable scenario (obtained in Step (k)), minimizing MOC_w shown in (7), and satisfying constraints shown in (8)–(11), (15)–(18), and (20)–(21).
- (m) An objective value needs to be assigned to each particle's position in the PSO algorithm. To this end, the objective value of total operation cost of the microgrid (shown in (5)) is calculated based on the optimal dispatches of microgrid resources procured in Steps (f) and (l).

- (n) Take the particles' position with the smallest objective value as the local best solution.
- (o) In the case of first iteration, take the local best solution obtained in Step (n) as the global best solution; otherwise, if the objective value of the local best solution is smaller than that of the global best solution, take the local best solution as the global best solution; otherwise do not change the global best solution.
- (p) Take the best set of DERs power factors obtained by the PSO (global best solution) and the associated hourly dispatch of microgrid resources obtained by the PDIP method as the desired solution.

3.3. MCVM method

In this section, a validation method called MCVM method is employed to benchmark the effectiveness of the proposed robust model for microgrid energy management against the stochastic one. The MCVM method is able to compare the proposed robust model versus the stochastic one with respect to their output (dispatches schedule of the microgrid resources), regardless of the employed scenarios in the models. In other words, MCVM method is able to compare two dispatches schedules (as shown in (38)) obtained by the robust and stochastic models, regardless of the way by which the schedules are obtained. To this end, the economic and security indices of the system are evaluated under N_{sc} random scenarios generated by the Mont Carlo simulation. In the robust and stochastic models, each of N_s most probable and dissimilar scenarios are considered once; while in the MCVM method N_{sc} scenarios are generated randomly in which most probable scenarios may be repeated several times with respect to their probabilities. In fact, in the MCVM method, the variables shown in (38)

are given; and the stochastic variables are determined satisfying constraints (8)–(11), (16)–(21), and (39). The load curtailment is just allowed under contingent scenarios. For each dispatches schedule, index of resources dispatching cost (RDC) is calculated by (40). RDC includes two parts: if the generated scenario is the non-contingent scenario which is the most probable scenario ($\beta_s^0 = 1$), the microgrid operation cost is computed as the first part; otherwise ($\beta_s^0 = 0$), it is calculated as the second part. Two dispatches schedules are compared based on the value of RDC index. In fact, the dispatches schedule with lower microgrid operation cost under the non-contingent scenario and lower cost of re-dispatching the microgrid resources under the contingent scenarios is more effective. Through the MCVm method, the dispatches schedule by which the system is more robust against the probable contingencies and needs less load curtailment and resources generation rescheduling, has more optimality.

$$[SR_{g,i,t}^0, PDIG_{g,i,t}^0, QDIG_{g,i,t}^0, PPV_{p,i,t}^0, QPV_{p,i,t}^0, PSUB_{i,t}^0, QSUB_{i,t}^0] \quad (38)$$

$$\max\{PDIG_{g,i}^{\min}, PDIG_{g,i,t}^0\} \leq PDIG_{g,i,t,s} \leq \min\{PDIG_{g,i}^{\max}, PDIG_{g,i,t}^0 + SR_{g,i,t}^0\}, \text{ if } \beta_{cs}^0 = 0, \quad (39)$$

$$\begin{aligned} \text{Min RDC} = & \frac{1}{N_{SC}} \sum_{s=1}^{N_{SC}} \sum_{t=1}^{N_T} \left(Ploss_{t,s} \cdot \rho loss_t + \beta_s^0 \sum_{i=1}^{N_B} \left(PSUB_{i,t}^0 \cdot \rho PSUB_{i,t} \right. \right. \\ & + QSUB_{i,t}^0 \cdot \rho QSUB_{i,t} + \sum_{p=1}^{NPV_i} PPV_{p,i,t}^0 \cdot \rho PV_{p,i,t} \\ & \left. \left. + \sum_{g=1}^{NDIG_i} (PDIG_{g,i,t}^0 \cdot \rho DIG_{g,i,t} + SR_{g,i,t}^0 \cdot \rho SR_{g,i,t}^0) \right) \right) \\ & + (1 - \beta_s^0) \sum_{i=1}^{N_B} \left(PSUB_{i,t,s} \cdot \rho PSUB_{i,t} + QSUB_{i,t,s} \cdot \rho QSUB_{i,t} \right. \\ & + \sum_{p=1}^{NPV_i} PPV_{p,i,t,s} \cdot \rho PV_{p,i,t} + \sum_{g=1}^{NDIG_i} PDIG_{g,i,t,s} \cdot \rho DIG_{g,i,t} \\ & \left. \left. + VOLL \cdot \sum_{k=1}^{N_K} \alpha_{k,i} \cdot LNS_{k,i,t,s}^p \right) \right) \quad (40) \end{aligned}$$

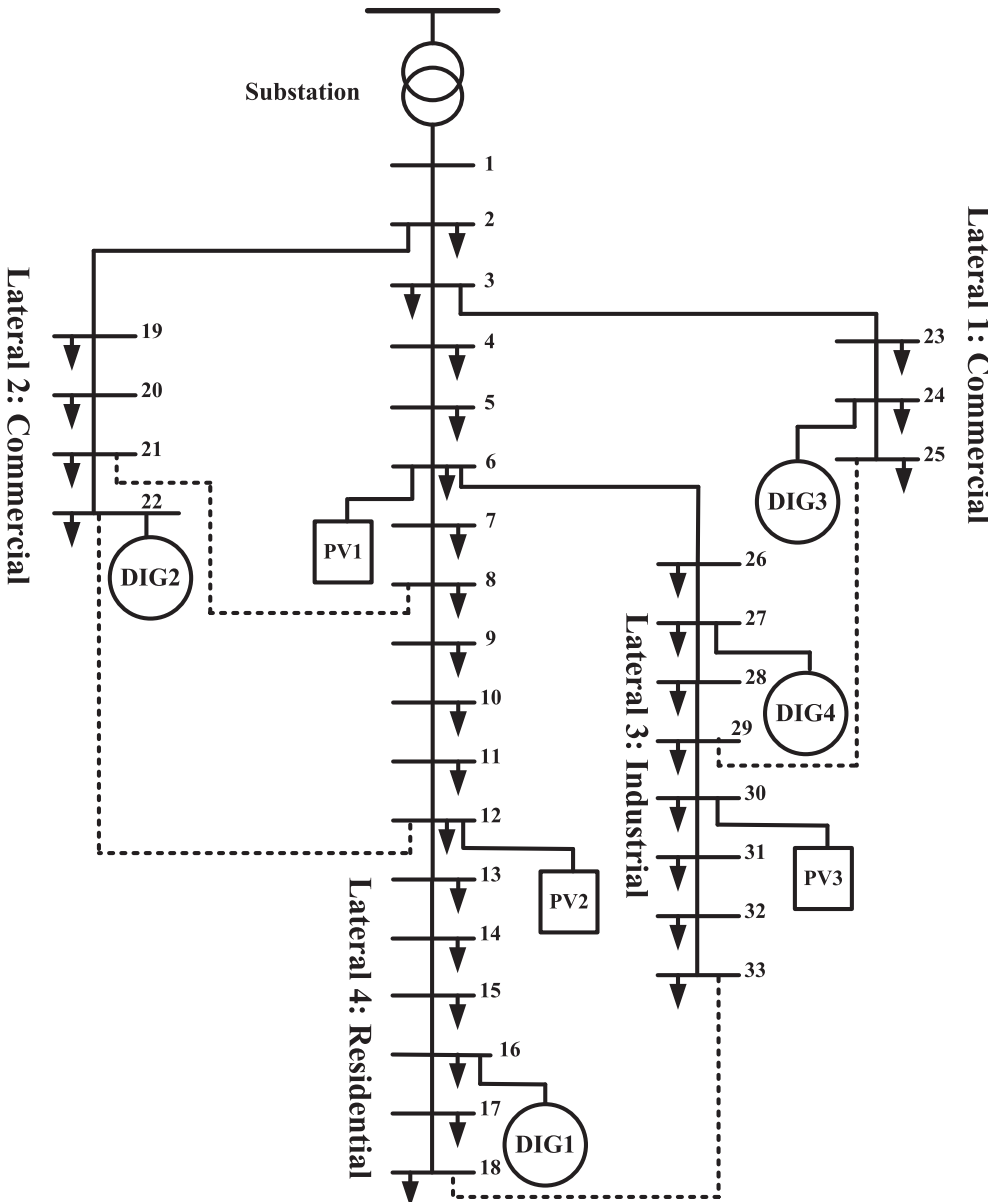


Fig. 6. Single line diagram of the modified IEEE 33-bus standard distribution system operating as a microgrid with variable PVs.

4. Numerical results

The proposed approach for optimal energy management of the microgrid is applied to a modified version of IEEE 33-bus standard distribution system converted into a microgrid with three variable PVs and four diesel generators [8]. Each PV has the capacity of 400 KW, while the capacity of each DIG is considered as 800 KW. As shown in Fig. 6, the system is connected to the main grid through a substation. It has five tie-lines (looping branches), and a peak demand of 3715 KW and 2300KVAR. The base values are considered as $S_{base} = 1000\text{KVA}$ and $V_{base} = 12.66\text{ kV}$. The various demands of the system i.e., residential, industrial and commercial customers have their own normalized daily load patterns, as shown in Fig. 7. The mean and standard deviation of insolation PDFs for each hour, as well as the characteristics of PV modules are considered as in [19]. Employing the proposed insolation forecast modeling, the normalized most probable (with no insolation error ($\sigma = 0$)) PV output for the 24-h period is obtained as depicted in Fig. 7. Operation and maintenance (O&M) cost of PVs and DIGs, and spinning reserves cost of DIGs are considered as 0.1095\$/KWh, 0.171\$/KWh and 0.087\$/KWh, respectively [36]. Cost of the active and reactive power supplied by the substation at the peak hour (Hour 21) are considered as 0.2\$/KWh and 0.11\$/KVarh, respectively. Normalized daily cost pattern for active and reactive power supplied by the substation is the same, and presented in Fig. 7 [36]. The value of lost load (VOLL) and cost of active power losses are considered equal to 0.7\$/KWh and 0.06\$/KWh, respectively [37]. Loads located on each bus are assumed to be of identical type (their importance factors are the same). $\alpha_{k,i}$ is considered equal to 100 for all the system buses.

The proposed method is implemented in MATLAB 7.11 software environment. Matlab Interior Point Solver (MIPS) which is a package of Matlab language M-files for solving NLPs using PDIP method, is employed to solve the sub-problem of optimal dispatches of the microgrid resources for each particles' position in PSO [38]. The solutions accuracy in the PSO algorithm depends on its initial parameters. Consequently, PSO runs several times to set the values of the initial parameters. Besides, the optimality of the solutions is improved by a local search around the procured solution. To demonstrate the effectiveness of the proposed robust model versus the traditional stochastic one, the proposed hybrid PSO algorithm and PDIP method versus the pure classic one (only PDIP method), and to evaluate the efficiency of the proposed VAR compensation mode utilization of grid-tie PV inverters versus the conventional utilization of the PVs, four cases are introduced in this section:

Case I: Robust energy management of the microgrid with VAR compensation mode of the PVs solved by the hybrid method

Case II: Robust energy management of the microgrid including PVs with unity PFs solved by the hybrid method

Case III: Stochastic energy management of the microgrid with VAR compensation mode of the PVs solved by the hybrid method

Case IV: Robust energy management of the microgrid with VAR compensation mode of the PVs solved by the PDIP method

4.1. Case I: proposed robust model

To detect the worst-case probable 24-h scenario, first 1000 random 24-h scenarios are generated among which 100 most probable ones are chosen as the final scenarios ($N_s = 100$). Then, the BDSG approach is applied to the proposed WCSD problems under these scenarios to detect the worst-case probable scenario. The aim is to obtain an efficient solution of BOP (26), which minimizes $|\mu_2(x) - m\mu_1(x)|$ over the Pareto frontier. Here, m is chosen as 1 which indicates that the importance of the second security objective (BLI) for the microgrid operator is the same as the importance of the first security objective (VD) ($w_1 = 1/2$, $w_2 = 1/2$). It is assumed that when a component encounters a failure, its repair takes five hours so that it can return to circuit. Outage of Line 1–2 at Hour 18 with the most probable daily PV output as shown in Fig. 7 (Scenario A) is detected as the worst-case probable scenario. Solving the energy management problem under the non-contingent scenario (with no insolation error and component outage) and the worst-case probable scenario (Scenario A), the hourly dispatches of microgrid resources are obtained as shown in Figs. 8 and 9. Total energy and reserves hourly dispatches of microgrid resources and the active power supplied by the substation for Case I are presented in Fig. 8. Fig. 9 depicts the reactive power dispatches of microgrid resources and the reactive power supplied by the substation for Case I. As shown in Fig. 8, the total scheduled spinning reserves is significantly increased during Hours 18–22 when Line 1–2 is faulted in worst-case scenario. Besides, it is seen from Fig. 8, the DIGs are almost fully contributed in energy and reserves provision during these hours. In fact, the dispatches of the microgrid resources are scheduled to be capable of withstanding Scenario A with minimum load curtailment and resources re-dispatching. Results show that resources dispatches schedule obtained by Case I is able to withstand Scenario A with no load curtailment. Furthermore, it can be seen from Fig. 8, active power outputs of microgrid resources (PVs and DIGs) are considerably increased during peak hours (Hours 11–15 and 19–22); the reason is that the cost of active power of substation is higher than the operation cost of the microgrid resources. As shown in Fig. 9, DIGs are scheduled to operate with almost unity power factors, except Hours 11–14 when the insolation level is high and thereby reactive power generation by PVs is low.

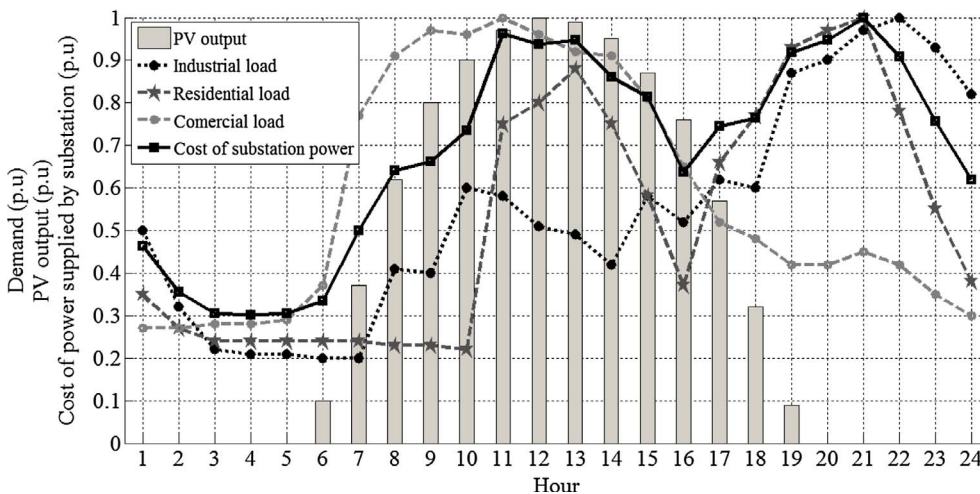


Fig. 7. Normalized most probable daily PV output, daily cost of power supplied by substation, and daily demand curve for various customers.

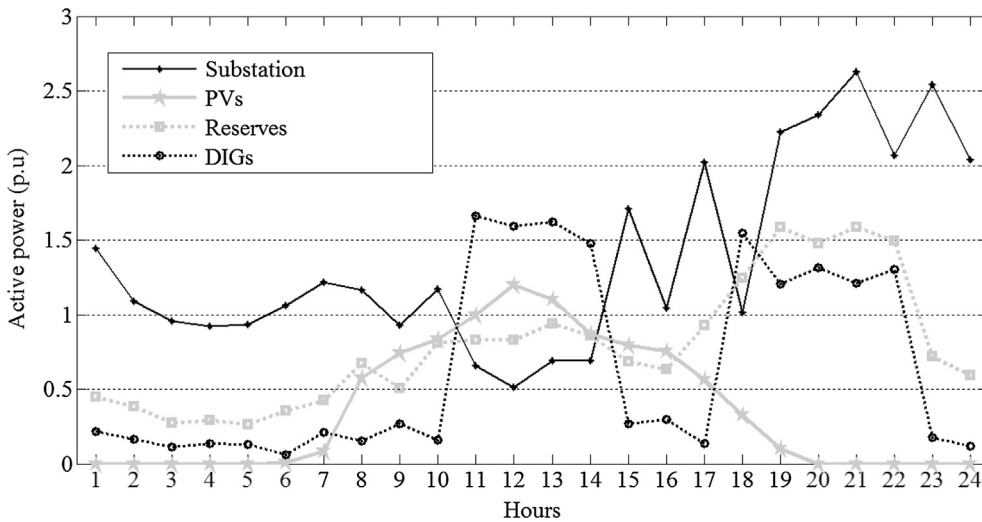


Fig. 8. Total reserves dispatches, and total active power supplied by microgrid resources and substation in Case I.

4.2. VAR compensation mode utilization versus the conventional utilization

To demonstrate the effectiveness of the proposed VAR compensation mode utilization of the PV inverters, two dispatches schemes of the microgrid resources for Cases I and II are evaluated in this section. In Case II, it is assumed that the PVs generate no reactive power. The objective results for the non-contingent scenario of Cases I and II, including the energy and reserves costs of microgrid resources, the cost of active and reactive power supplied by the substation, and the cost of active power losses, are presented in Table 1. As shown in Fig. 9, the RPCF available by PV inverters is utilized to supply a significant part of reactive demand when the insolation is weak, especially during nightly peak hours (Hours 19–23) when the cost of reactive power supplied by the substation is high. That is why the total cost of reactive power by the substation is decreased by 60.71% from Case II to Case I (as shown in Table 1). Besides, as shown in Fig. 8, active power outputs of PVs are increased during Hours 11–13 when the insolation level and the costs of active power supplied by the substation are high. Because of this and due to reduction of reactive power supplied by the substation, the total operation cost of the microgrid (MOC_n) is decreased by 7.17% from Case II to Case I (as shown in Table 1). It is also concluded from Table 1 that the total active power loss is decreased by 6.09% from Case II to Case I.

4.3. Sensitivity analysis

In order to evaluate the sensitivities of the economic and security indices of the microgrid to deviation in the generation dispatch of DERs (PVs and DIGs), a sensitivity analysis is performed. The sensitivity of the microgrid operation cost (MOC) to small deviation in the active power generation dispatch of DER d from the microgrid operating point under non-contingent scenario is procured by (41) using the first order approximation of Taylor series for the microgrid operation cost. Each sensitivity is approximated considering the linear relationship between the microgrid operation cost and the dispatch of each DER [39].

$$S_{PDER_d}^{MOC} = \frac{\partial MOC}{\partial PDER_d} \approx \frac{\Delta MOC}{\Delta PDER_d} = \frac{MOC_1 - MOC_0}{\Delta PDER_d} \quad (41)$$

where, MOC_0 is the microgrid operation cost in the non-contingent scenario and MOC_1 shows the microgrid operation cost after small deviation in active power generation dispatch of DER d ($\Delta PDER_d$). Similarly, the sensitivities of indices voltage deviation (VD) and branches loading index (BLI) to deviation in the active and reactive power generation dispatch of DER ($S_{PDER_d}^{VD}, S_{PDER_d}^{BLI}, S_{QDER_d}^{VD}, S_{QDER_d}^{BLI}$) are calculated. The microgrid economic and security indices sensitivities are presented in Table 2.

As shown in Table 2, the sensitivity of microgrid operation cost with respect to active power generation dispatch of PVs is negative while the

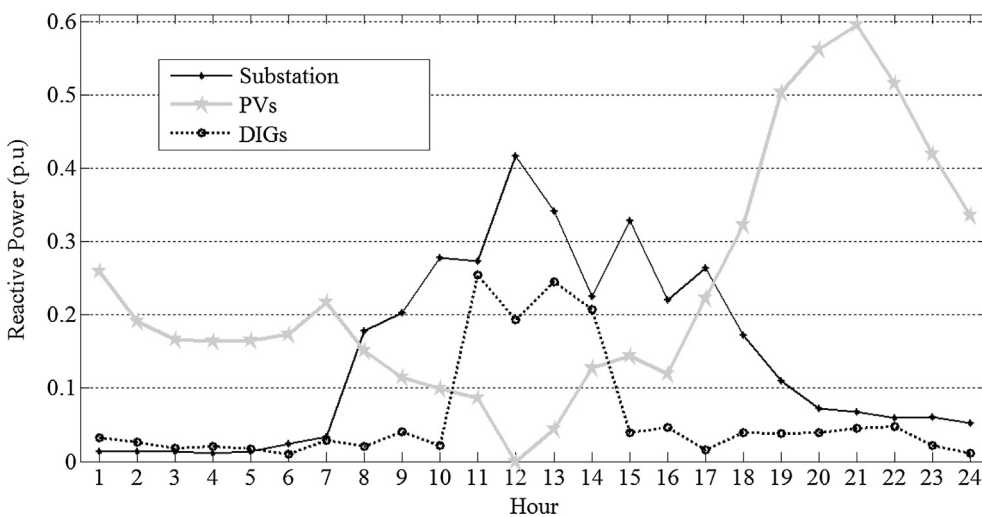


Fig. 9. Total reactive power supplied by microgrid resources and substation in Case I.

Table 1
Operation costs for the non-contingent scenario of Cases I, II and III.

Case	PVs energy cost (\$)	DIGs		Cost of active power of substation (\$)	Cost of reactive power of substation (\$)	Cost of active loss (\$)	Total (\$)
		Reserves cost (\$)	Energy cost (\$)				
Case I	981	1639	2656	4744	308	108	10433
Case II	1006	1943	2031	5360	784	115	11239
Case III	1035	1328	2653	4685	318	102	10121

Table 2
Sensitivities of the economic and security indices of the microgrid to deviation in the active and reactive power generation dispatch of DERs at daily peak hour (Hour 11) for Case I.

DERs	$S_{PDER_d}^{MOC}$	$S_{PDER_d}^{VD}$	$S_{PDER_d}^{BLI}$	$S_{QDER_d}^{MOC}$	$S_{QDER_d}^{VD}$	$S_{QDER_d}^{BLI}$
	(\$/KW)	(kV/KW)	(MVA/KW)	(\$/KVAh)	(kV/KVAh)	(MVA/KVAh)
PV1	-12.74	0.0167	-0.6904	-3.597	-0.0789	-0.1849
PV2	-19.64	0.0174	-0.531	-6.116	-0.0817	0.1697
PV3	-15.21	-0.0119	-0.6915	-5.486	-0.0812	-0.173
DIG1	8.03	0.0155	-0.6888	-6.34	-0.0689	-0.2208
DIG2	6.73	0.0117	-0.5957	-4.79	-0.0781	0.2124
DIG3	13.11	-0.013	-0.6579	-1.628	-0.0611	0.1875
DIG4	4.36	-0.0149	-0.5279	-5.777	-0.0799	0.2292
Substation	38.93	0.0197	0.8311	18.63	-0.0563	-0.1689

sensitivity of the microgrid operation cost with respect to active power generation dispatch of diesel generators is positive. This is due to relatively high O&M cost of diesel generators. The sensitivity of the microgrid operation cost with respect to reactive power generation dispatch of PVs and diesel generators is negative. This is because of reduction of the reactive power supplied by the substation by producing the reactive power by PVs and DIGs. The sensitivity of BLI index with respect to active power generation dispatch of PVs and DIGs is negative, while with respect to active power generation dispatch of the substation is positive. This means that active power generation by PVs and DIGs reduces the loading percentage of the branches, while the active power generation by the substation increases it. Furthermore, Table 2 shows the impacts of reactive power generation by DIGs and PVs on improving the voltage profile of the microgrid.

4.4. Robust model versus stochastic model

In this section, proposed MCVM method is employed to benchmark the effectiveness of the proposed robust model for microgrid energy management (Case I) against the stochastic model proposed in [30] (Case III). For the fair comparison, in the stochastic model, 1000 random 24-h scenarios are generated among which 100 most probable ones are employed as the final scenarios. The problem of the microgrid energy management is solved under these final scenarios. In the stochastic model, the most likely scenarios are used, while the worst-case probable scenario causing maximum indices of VD and BLI, is employed in the proposed robust model. MCVM method is able to compare two dispatches schedules (as shown in (38)) obtained by the robust and stochastic models, regardless of the scenarios under which the schedules are obtained. To this end, the economic and security indices of the system are evaluated under 1000 random scenarios generated by the Mont Carlo simulation ($N_{SC} = 1000$). 100 final most probable scenarios employed in robust and stochastic models are repeated several times with respect to their probabilities, so that they consist about 71.2% of 1000 generated scenarios. The non-contingent scenario with no insolation error and component outage which is the most probable scenario is repeated 320 times. As shown in Table 1, energy and reserves costs are increased in Case I in compared to Case III, to withstand the worst-case scenario with optimized objectives (total operation cost is increased by 3.08% from Case III to Case I). Economic and security indices obtained by

Table 3
Economic and security indices obtained by the MCVM method for Cases I and III.

Case	RDC (\$)	AENS (p.u)	AVD (p.u)	ABLI (p.u)	Solution time (s)
Case I	15918	5.11	14.25	707.63	1542
Case III	18053	7.26	17.42	737.28	2324
Case IV	19332	6.9	20.08	745.91	974

the MCVM method for Case I and III are presented in Table 3. These indices include resources re-dispatching cost (RDC), average energy not supplied ($AENS = \frac{1}{N_{SC}} \sum_{s=1}^{N_{SC}} \sum_{t=1}^{N_T} \sum_{i=1}^{N_B} \sum_{k=1}^{N_K} LNS_{k,i,t,s}^P$), average voltage deviation ($AVD = \frac{1}{N_{SC}} \sum_{s=1}^{N_{SC}} VD_s$), and average branches loading index ($ABLI = \frac{1}{N_{SC}} \sum_{s=1}^{N_{SC}} BLI_s$). As shown in Table 3, the load curtailments to withstand the contingencies are significantly decreased in Case I in compared to Case III (AENS is decreased by 29.61% from Case III to Case I). That is why although the operation cost under non-contingent scenario is increased in Case I in compared to Case III (see Table 1), the index of RDC is decreased by 11.83% from Case III to Case I. This demonstrates more optimality of the dispatches schedule of the microgrid resources obtained by the robust model in compared to that of the stochastic model. The reason is that in the stochastic model, share of each scenario in the expected values of the objectives is computed with respect to the normalized value of that scenario probability. This does not guarantee the optimal optimization of the objective functions in the mathematical optimization scenario-based problem. Besides, the security indices of AVD and ABLI are compared between two Cases I and III in Table 3. As shown in this table, indices of AVD and ABLI are decreased by 18.19% and 4.02% in Case I in compared to Case III. This is due to integration of these security indices into the objectives of WCSD problems in the proposed robust model. In fact, in the robust model, the resources dispatches are scheduled to optimize the economic objective under the contingent scenario with the severest effects on the security indices of voltage profile and branches loading index. This leads to more robust solution in compared to the stochastic model, as shown in Table 3. To more analysis, the operational performances of resources dispatches schedules obtained by Cases I and III are compared under a scenario corresponding to outage of Line 2–3 at Hour 11 with the same most probable daily PV output shown in Fig. 7 (Scenario B). This scenario is not included in either 100 final scenarios of the robust model or 100 final scenarios of the stochastic model. No load curtailment is allowed in solving the energy management problem of both cases under the contingent Scenario B. The results show that the optimization does not converge to a solution for Case III, while Case I is able to withstand this contingency without any load curtailment. This is because some variables such as the flow of lines and the buses voltages violate their limits in Case III.

Voltage profile of the system buses under contingent Scenario B, at Hour 15 is compared between Cases I and III in Fig. 10. As shown in this figure, the voltage profile of the system buses is significantly improved in Case I in compared to Case III. The voltages of Buses 17, 18 and 32 in Case III violate the lower limit (0.95 p.u), while in Case I, all the buses voltages satisfy their limits. The reason is that the stochastic model may not provide sufficient security level to find a more economical solution. This is while, the resources dispatches schedule obtained by Case I is able to withstand all the contingent scenarios employed in the stochastic model, since it is procured to maintain the system security

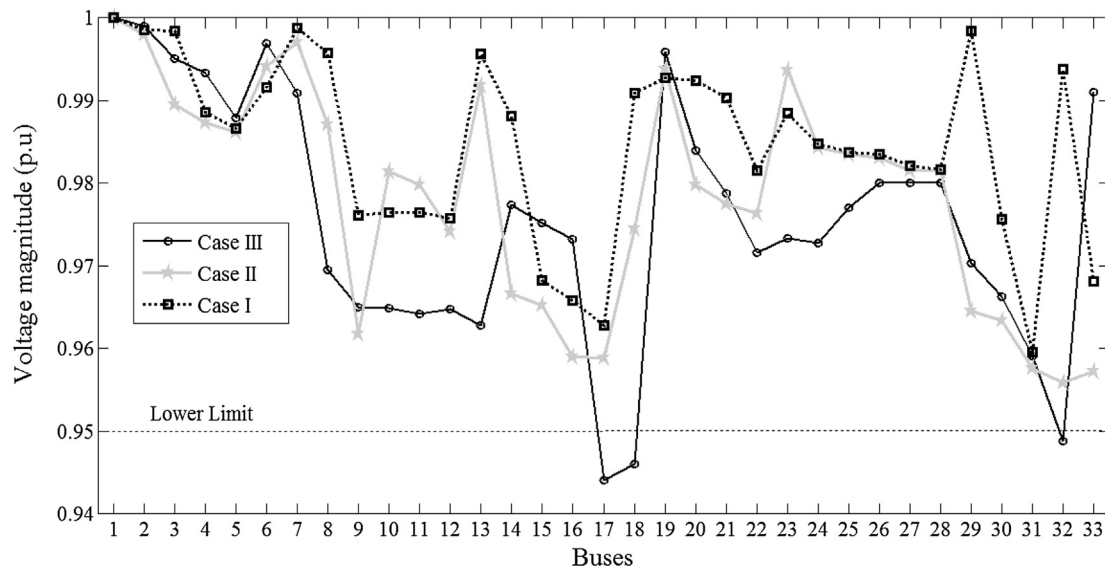


Fig. 10. Voltage profile at Hour 15 for all cases under contingent Scenario B.

against the worst-case event. Consequently, the dispatches schedule obtained by the robust model is more likely to withstand a contingency out of the final scenarios considered to procure the schedule. Furthermore, as presented in Table 3, the computational burden is significantly decreased in Case I in compared to Case III. Voltage profile of the test system at Hour 15, under contingent Scenario B are also compared between Cases I and II in Fig. 10. In this hour, the total active and reactive power outputs of PVs in Case I are 0.79 p.u. and 0.14 p.u., respectively, while the PVs are just generating 0.84 p.u. active power in Case II. As shown in Fig. 10, the voltages profile of the system buses is significantly improved in Case I in compared to Case II due to the RPCF capability provided by the PVs' inverters.

4.4. Hybrid method versus pure classic method

To benchmark the efficiency of the proposed hybrid PSO algorithm and PDIP method (Case I) versus the pure classic PDIP method (Case IV) for the robust energy management of the microgrid, MCVM method, as explained in Section 4.4, is employed to compare the dispatches schedules obtained by both cases by evaluating the economic and security indices of the system under 1000 generated random scenarios. In contrast to Case I, in Case IV, all decision variables including the dispatches of the energy and reserves resources and optimal PFs of DERs, as well as active and reactive power supplied by the substation are determined as the scenario dependent decision variables by the PDIP method. Then, the aggregated solution is obtained by the expected value operator. As shown in Table 3, although the number of decision variables are increased in Case IV in compared to Case I, the computational burden is decreased by 36.83%. This is due to relatively high computational cost of the PSO algorithm in Case 1. However, as shown in Table 3, the indices of RDC, AENS, AVD, and ABLI are increased by 21.45%, 35.03%, 40.91%, and 5.41%, from Case I to Case IV, respectively. This is because in case I some decision variables including the dispatches of the reserves resources and optimal PFs of DERs are defined as scenario independent variables which are obtained by the PSO algorithm. These variables act as constant parameters in the NLP problem solved by the PDIP method. This reduces the complexity and nonlinearity of the optimization problem, and eliminates the need for a scenario aggregation approach which decreases the solution optimality in Case IV.

It is to be noted that, the studied test system acts as a realistic test case which is close to real-world network specification. Therefore, the proposed robust model which is evaluated and validated based on the studies on this test system, can be generalized to any large-scale real-

world microgrid with the cost of higher computation burden. The proposed robust optimization problem takes 25 min and 42 s of CPU time using serial computation on a personal computer with CPU-2.6 GHz Core i5 and 4 GB RAM, as shown in Table 3. In other words, all scenarios are sequentially solved on this personal computer. As the proposed robust energy management model is well-suited for parallel processing computer systems, computation time can be significantly decreased. Besides, some simplifications are made for mitigating the dimensionality issue. Furthermore, it is noted that the provided results for the robust microgrid energy management are outcomes of prototype software executed on a simple hardware set in our lab, since the main focus is on presenting the underlying ideas. To procure an industrial software package from a prototype computer code, different software techniques are usually employed to optimize the written code by improving its computation burden and memory usage. Moreover, microgrid operators are usually equipped with much powerful computers for energy management process than our simple hardware set.

In hierarchical architecture of grid-tied microgrids, the local controllers of the energy resources are governed by a central controller [40]. Efficiency and reliability of microgrid control and operation are recently enhanced with the advancement of computer communication technologies and smart meters in smart grids. SCADA is one of these communication technologies which facilitates the control, configuration and supervision of the microgrids [41]. The solution obtained by the proposed robust energy management model provides a new hourly strategy for the central controller of the microgrid to govern the local controllers of the energy resources. To implement the proposed energy management model in the field, first the proposed optimization problem is solved considering the relevant constant parameters of the microgrid including physical parameters, operational parameters of the energy sources and associated cost values. Then the obtained hourly dispatches schedule of the energy and reserves resources is implemented by the central controller of the microgrid to govern the local controllers of the energy sources using SCADA elements.

5. Conclusion

In this paper, an effective model was presented for the robust energy management of the microgrid considering VAR compensation mode of the PV inverters. In the proposed model, first, the worst-case scenario with the severest effects on the system security is detected among the probable scenarios. To this end, a bi-objective energy management problem maximizing the indices of VD and BLI are solved under the

probable scenarios. After detection of the worst-case probable scenario, the main energy management problem of the microgrid is solved under this scenario, minimizing the microgrid operation cost. The hybrid PSO algorithm and PDIP method is employed to solve the proposed microgrid energy management problem. Proposed MCVM method is employed to evaluate the effectiveness of the proposed robust model versus the stochastic one, and the proposed hybrid method versus the pure classic method (only PDIP method). Besides, the effectiveness of the RPCF capability provided by the PVs' inverters is verified against the conventional utilization of the PVs. The following results were concluded:

- Although the resources dispatches schedule obtained by the proposed robust model leads to higher microgrid operation cost under the non-contingent scenario in compared to that of the stochastic model, results of the MCVM method throughout 1000 real world scenarios demonstrate that the dispatches schedule obtained by the proposed robust model is generally more optimal than that of the stochastic model and leads to lower re-dispatching cost under generated scenarios.
- The stochastic model may not provide sufficient security level to find a more economical solution, and a robust model based on the worst-case probable scenario is required to ensure the system security against the probable severe contingencies. The resources dispatches schedule obtained by the robust model is more likely to withstand a contingency out of the final scenarios considered to procure the schedule. Besides, the robust model leads to lower computational burden.
- Combining the features of both classic and heuristic methods which reduces the complexity and nonlinearity of the microgrid energy management optimization problem and eliminates the need for a scenario aggregation approach increases the solution optimality in compared to the pure classic method.
- RPCF capability provided by the inverters significantly reduces total operation cost of the microgrid by decreasing the reactive power supplied by the substation, especially at nightly peak hours when the insolation level is low and the cost of reactive power supplied by the substation is high.

References

- [1] Varma RK, Das B, Axente I, Vanderheide T. Optimal 24-hr utilization of a PV solar system as STATCOM (PV-STATCOM) in a distribution network. In: IEEE Power and Energy Society General Meeting, July 2011.
- [2] Hengsratawat V, Tayjasanant T, Nimpitiwan N. Optimal sizing of photovoltaic distributed generators in a distribution system with consideration of solar radiation and harmonic distortion. *Int J Electr Power Energy Syst* 2012;39(1):36–47.
- [3] Granaghan MM, Houseman D, Schmitt L, Cleveland F, Lambert E. Enabling the integrated grid: leveraging data to integrate distributed resources and customers. *IEEE Power Energy Mag* 2016;14(1):83–93.
- [4] Bazrafshan MH, Gatsis N. Decentralized stochastic optimal power flow in radial networks with distributed generation. *IEEE Trans Smart Grid* 2016. In press.
- [5] Tan S, Xu J, Kumar Panda S. Optimization of distribution network incorporating distributed generators: an integrated approach. *IEEE Trans Power, Syst* 2013;28(3):2421–32.
- [6] Hernandez JC, Medina A, Jurado F. Optimal allocation and sizing for profitability and voltage enhancement of PV systems on feeders. *Renew Energy* 2007;32(10):1768–89.
- [7] Wen Sh, Lan H, Fu Q, Yu DC, Zhang L. Economic allocation for energy storage system considering wind power distribution. *IEEE Trans Power Syst* 2015;30(2):644–52.
- [8] Jain N, Singh SN, Srivastava SC. A generalized approach for DG planning and viability analysis under market scenario. *IEEE Trans Ind Electron* 2013;60(11):5075–85.
- [9] Silvestre MLD, Graditi G, Sanseverino ER. A generalized framework for optimal sizing of distributed energy resources in micro-grids using an indicator-based swarm approach. *IEEE Trans Ind Inf* 2014;10(1):152–62.
- [10] Basu AK, Bhattacharya A, Chowdhury S, Chowdhury SP. Planned scheduling for economic power sharing in a CHP-based micro-grid. *IEEE Trans Power Syst* 2012;27(1):30–8.
- [11] Abbasi F, Hosseini SM. Optimal DG allocation and sizing in presence of storage systems considering network configuration effects in distribution systems. *IET Gener Transm Distrib* 2016;10(3):617–24.
- [12] Alnaser SW, Ochoa LF. Optimal sizing and control of energy storage in wind power-rich distribution networks. *IEEE Trans Power Syst* 2016;31(3):2004–13.
- [13] Arefifar SA, Abdel-Rady Y, Mohamed I. Probabilistic optimal reactive power planning in distribution systems with renewable resources in grid-connected and islanded modes. *IEEE Trans Ind Electron* 2014;61(11):5830–9.
- [14] Bueno PG, Hernández JC, Ruiz-Rodríguez FJ. Stability assessment for transmission systems with large utility-scale photovoltaic units. *IET Renew Power Gener* 2016;10(5):584–97.
- [15] Hernández JC, Bueno PG, Sanchez-Sutil F. Enhanced utility-scale photovoltaic units with frequency support functions and dynamic grid support for transmission systems. *IET Renew Power Gener* 2017;11(3):361–72.
- [16] Mokryani G, Majumdar A, Pal BC. Probabilistic method for the operation of three-phase unbalanced active distribution networks. *IET Renew Power Gener* 2016;10(7):944–54.
- [17] Dall'Anese E, Dhople SV, Giannakis GB. Optimal dispatch of photovoltaic inverters in residential distribution systems. *IEEE Trans Sustain Energy* 2014;5(2):487–97.
- [18] Tonkoski R, Turcotte D, EL-Fouly THM. Impact of high PV penetration on voltage profiles in residential neighborhoods. *IEEE Trans Sustain Energy* 2012;3(3):518–27.
- [19] Hung DQ, Mithulananthan N, Lee KY. Determining PV penetration for distribution systems with time-varying load models. *IEEE Trans Power Syst* 2014;29(6):3048–57.
- [20] Ruiz-Rodríguez FJ, Hernández JC, Jurado F. Voltage unbalance assessment in secondary radial distribution networks with single-phase photovoltaic systems. *Int J Electr Power Energy Syst* 2015;64:646–54.
- [21] Braun M. Provision of ancillary services by distributed generators: technological and economic perspective. Kassel, Germany: Kassel University Press GmbH; 2009.
- [22] Sarshar J, Moosapour SS, Joorabian M. Multi-objective energy management of a micro-grid considering uncertainty in wind power forecasting. *Energy* 2017. In press.
- [23] Dehimi A, Keshavarz Zahed B, Irvani R. An interactive operation management of a micro-grid with multiple distributed generations using multi-objective uniform water cycle algorithm. *Energy* 2016;106:482–509.
- [24] Wang L, Li Q, Ding R, Sun M, Wang G. Integrated scheduling of energy supply and demand in microgrids under uncertainty: a robust multi-objective optimization approach. *Energy* 2017;130:1–14.
- [25] Sukumar Sh, Mokhlis H, Mekhilef S, Naidu K, Karimi M. Mix-mode energy management strategy and battery sizing for economic operation of grid-tied microgrid. *Energy* 2017;118:1322–33.
- [26] Barelli L, Bidini G, Bonucci F. A micro-grid operation analysis for cost-effective battery energy storage and RES plants integration. *Energy* 2016;113:831–44.
- [27] Bahmani-Firouzi B, Azizipahan-Abarghoee R. Optimal sizing of battery energy storage for micro-grid operation management using a new improved bat algorithm. *Int J Electr Power Energy Syst* 2014;56:42–54.
- [28] Niknam T, Azizipahan-Abarghoee R, Narimani MR. An efficient scenario-based stochastic programming framework for multi-objective optimal micro-grid operation. *Appl Energy* 2012;99:455–70.
- [29] Diwekar U. Optimization under uncertainty: an overview. *SIAG/OPT views-and-news* 2002;13(1):1–8.
- [30] Amjady N, Aghaei J, Shayanfar HA. Stochastic multiobjective market clearing of joint energy and reserves auctions ensuring power system security. *IEEE Trans Power Syst* 2009;24(4):1841–54.
- [31] Goroohi Sardou I, Khodayar ME, Khaledian K, Soleimanidamaneh M, Ameli MT. Energy and reserve market clearing with microgrid aggregators. *IEEE Trans Smart Grid* 2016;7(6):2703–12.
- [32] Hassaine L, Olias L, Quintero E, Haddadi M. Digital power factor control and reactive power regulation for grid-connected photovoltaic inverter. *Renew Energy* 2009;34(1):315–21.
- [33] Albuquerque FL, Moraes AJ, Guimaraes GC, Sanhueza SMR, Vaz AR. Photovoltaic solar system connected to the electric power grid operating as active power generator and reactive power compensator. *Sol Energy* 2010;84(7):1310–7.
- [34] Goroohi Sardou I, Khodayar ME, Ameli MT. Coordinated operation of natural gas and electricity networks with microgrid aggregators. *IEEE Trans Smart Grid*; 2016, PP (99): 1–1.
- [35] Potra FA, Wright SJ. Interior-point methods. *J Comput Appl Math* 2000;124(1–2):281–302.
- [36] Nikmehr N, Najafi-Ravadanegh S. Optimal operation of distributed generations in micro-grids under uncertainties in load and renewable power generation using heuristic algorithm. *IET Renew Power Gen* 2015;9(8):982–90.
- [37] Ali ES, Abd Elazim SM, Abdelaziz AY. Improved harmony algorithm and power loss index for optimal locations and sizing of capacitors in radial distribution systems. *Int J Electr Power Energy Syst* 2016;80:252–63.
- [38] Zimmerman RD, Murillo-Sanchez CE. In: *Matpower 4.1 User's Manual*, [Online]. Available at: <http://www.pserc.cornell.edu/matpower/manual.pdf>; 2017.
- [39] Aghaei J, Amjady N. A scenario-based multiobjective operation of electricity markets enhancing transient stability. *Int J Electr Power Energy Syst* 2012;35:112–22.
- [40] Álvarez E, Campos A, García R. Scalable and usable web based supervisory and control system for micro-grid management. In: *International Conference on Renewable Energies and Power Quality*, Granada, Spain, March 2010.
- [41] Pourbabak H, Chen T, Zhang B, Su W. Control and energy management system in microgrids. In: *Book "Clean energy microgrids"*, Stevenage, England, The Institution of Engineering and Technology; 2017, CH. 3.